Wave scattering by narrow cracks in ice sheets floating on water of finite depth

By D.V. EVANS AND R. PORTER
School of Mathematics, University of Bristol, Bristol, BS8 1TW, UK

(Received 07 August 2002)

An explicit solution is provided for the scattering of an obliquely-incident flexural-gravity wave by a narrow straight-line crack separating two semi-infinite thin elastic plates floating on water of finite depth. By first separating the solution into the sum of symmetric and anti-symmetric parts it is shown that a simple form for each part can be derived in terms of a rapidly-convergent infinite series multiplied by a fundamental constant of the problem. This constant is itself simply determined by applying an appropriate edge condition. Curves of reflection and transmission coefficients are presented showing how they vary with plate properties and angle of incidence. It is also shown that in the absence of incident waves and for certain relations between their wavelength and frequency, symmetric edge waves exist which travel along the crack and decay in a direction normal to the crack.

1. Introduction

In this paper we consider the scattering of obliquely-incident waves by a narrow straight-line crack separating two semi-infinite thin elastic plates floating on water of finite depth. A number of authors have considered related problems since they are important in considering the effect of large ice floes on ocean wave propagation in the South Atlantic. For a general review see Squire *et al* (1995). Also, more recently, such problems have become relevant to the possible construction of large floating runways for use in Japan, where the effect of bending of such large structures cannot be ignored.

An early solution for the scattering of acoustic waves propagating through a half-space containing a compressible fluid bounded by the two thin elastic plates having different properties separated by the crack is provided by Kouzov (1963a). He makes use of an integral representation which enables the problem to be reduced to a Riemann-Hilbert problem which he solves explicitly, it being equivalent to a Wiener-Hopf formulation. In a subsequent paper (Kouzov 1963b) he assumes the plates have identical properties.

One of the earliest related problems to be considered was the reflection and transmission of waves obliquely-incident from an open sea region by a single semi-infinite thin elastic plate in finite water depth. Thus, unaware of the work of Kouzov, Evans & Davies (1968) in an unpublished report used the Wiener-Hopf technique to obtain an explicit solution of the resulting boundary-value problem in terms of two constants which were determined in terms of the conditions of zero bending moment and shear stress assumed to be satisfied at the edge of the plate. Because of the complicated nature of the solution no numerical calculations were made and the authors resorted to a shallow-water solution from which the refection and transmission coefficients were computed.

A number of authors have revisited the semi-infinite elastic plate problem since often using the Wiener-Hopf approach. An exception to this is the sequence of papers by Squire

(1994a,b,c,d) in which he considered a wide range of different ice conditions and resulting dispersion equations although he was forced to neglect the local evanescent wave fields in order to make progress. In a major series of papers, Fox & Squire (1990,1991,1994) considered the full hydrodynamic equations including the local effects. They replaced the conditions of continuity of potential and horizontal velocity across the common water region under the edge of the plate by minimising numerically integrals over the depth of the square of the differences in potential and horizontal velocity whilst satisfying the edge boundary conditions. They were able to obtain a wide range of numerical results including the variation of reflection coefficient with angle of incidence and ice thickness (Fox & Squire 1994). A different approach has been made to the problem by Sahoo *et al* (2000). They use non-orthogonal eigenfunction expansions to obtain infinite systems of equations which they solve by truncation. However it is not clear how they eliminate certain constants which appear. Further modifications to the methods of Fox & Squire (1994) and Sahoo *et al* (2000) are made by Teng *et al* (2001).

More recently Balmforth & Craster (1999) and Chung & Fox (2000) have revisited the problem using the Wiener-Hopf method adopted by Evans & Davies (1968). In each of these papers the authors introduced ideas which enable numerical results to be obtained once the unknown constants have been determined from the edge conditions. Chakrabarti (2000), in considering the two-dimensional problem in infinitely deep water, reduced the problem to solving a Carlemann type of singular integral equation which he solved explicitly. Despite the author's claim to the contrary, the method provides no obvious reduction in complexity from the Wiener-Hopf approach although numerical results are obtained. In a very recent series of papers, Tkacheva (2001a,b,c) considers the problem for normally-incident waves only in both finite and infinite water depth, and obtains a remarkable simplification in the calculation of the constants resulting in the modulus of the reflection coefficient being expressible as the ratio of the difference to the sum of the wavenumbers in the open sea and in the elastic plate.

Acoustic scattering by a crack of finite width separating two thin elastic plates in infinite depth of compressible fluid has been considered by Andronov *et al* (1996). No explicit solution exists in this case and the authors reduce the problem to an integral equation for the potential across the crack using an appropriate Green's function. This is then solved numerically using a variant on the Galerkin method.

The particular problem studied here is easier than the ones described above and can be solved explicitly. However, like Kouzov many later authors have generalised the problem to allow the plates separated by the crack to have different properties and this is best approached by the Wiener-Hopf method. For example, Marchenko, first in finite depth (1993), and then in infinite depth (1997a), allows the plates to have different thicknesses and assumes a general stress-tensor in the plates to give a general dispersion relation for wave propagation. In each case the results are sketchy although some numerical results are presented. A clearer description of the solution and results, for deep water, is given in Marchenko (1999) whilst in Marchenko (1997b) the shallow water equations are used to solve the problem when the crack has finite dimensions. A recent approach to the crack problem is due to Squire & Dixon (2000) who use an appropriate Green's function in deep water to obtain simple expressions for the reflection and transmission coefficients when the plates have identical properties.

The approach we use here has much in common with Squire & Dixon's work, but differs in some important aspects. The difficulty with all such problems is the higher-order conditions to be satisfied at the edge of each plate. However, because of the symmetry of the problem we can split the solution into the sum of even and odd solutions each of which needs to satisfy one condition at one edge since then both the second condition at that edge and the two conditions at the other edge in this symmetric part of the solution are automatically satisfied by symmetry arguments. An explicit result for the symmetric potential then results from applying Green's identity to an appropriate symmetric Green's function and the unknown symmetric potential. Thus the solution turns out to be a single known series multiplied by a constant, P_s, which is related to the slope of the edge of the plate. Satisfaction of the zero bending moment condition then determines P_s. Likewise the solution of the anti-symmetric part, utilising an appropriate anti-symmetric Green's function, turns out to be a known series multiplied by a constant, Q_a, which is related to the displacement of the edge of the plate. Satisfaction of the zero shear stress condition now determines Q_a. Note that despite the vanishing of certain higher derivatives defining the shear stress and bending moment at both edges, neither P_s nor Q_a is continuous across the crack.

There are two other ways in which our approach differs from that of Squire & Dixon (2000). First we allow obliquely-incident waves to be scattered by the crack. This provides no major added difficulty apart from a more complicated pair of edge conditions to be satisfied by each plate. However, it does allow for the possibility, which we address, of the existence of localised edge waves travelling along the crack in the absence of incident waves which do not radiate energy away from the crack. This can occur if the wavenumber of such waves is large enough so that waves cannot radiate to and from infinity.

Secondly, we assume finite water depth. This enables us to make a fresh approach to the problem by expanding the solutions in the water region beneath each plate in a series of eigenfunctions each term of which corresponds to a root of the dispersion relation. In seeking to match the expansions across the common region beneath the crack, we make use of a non-orthogonal condition first introduced by Lawrie & Abrahams (1999) and applied to a related problem (Lawrie & Abrahams 2002) which is shown to be satisfied by the eigenfunctions. Again symmetric and anti-symmetric solutions are sought and the resulting series expressions are shown to agree with those obtained by the Green's function approach. This is important as it demonstrates that the assumed expansions in a series of eigenfunctions corresponding to all the roots of the dispersion relation is in fact complete and hence justified thereby paving the way to using such non-orthogonal expansions in similar problems in finite depth where an explicit solution is not available.

The lay-out of the paper is as follows. The mathematical problem is formulated in the next section and includes a description of the separation into symmetric and anti-symmetric parts and its implications. The solution using Green's functions is derived in section 3 whilst in section 4 the shorter eigenfunction expansion method of solution is derived. A brief section 5 presents the conditions for the existence of localised waves travelling along the crack. The results are presented in section 6 where curves of reflection and transmission coefficients are sketched as functions of wave incident angle, wave frequency and plate geometry. Throughout the paper careful attention is paid to convergence matters which are considered in the Appendix where a number of identities are also proved.

2. Formulation and preliminaries

Consider the following problem. Fluid occupies the region $-h < y < 0$, $-\infty < x, z < \infty$ which is bounded by a rigid bottom $y = -h$ and the free surface $y = 0$ on which there are floating two semi-infinite thin elastic plates separated only by an infinitely-long crack of negligible width defined by $x = y = 0$, $-\infty < z < \infty$. At $x = y = 0$ the plates are free so that both the shearing stress and bending moment vanish. We seek the reflection and transmission coefficients when a plane wave propagating along one of the plates is obliquely-incident from $x = \infty$ on the junction between the plates. Under the assumptions of linearised theory we seek a velocity potential $\Phi_t(x, y, z, t)$ in the region $-\infty < x, z < \infty$ and look for a solution ϕ_t where

$$\Phi_t(x, y, z, t) = \Re\{\phi_t(x, y)\mathrm{e}^{ilz - i\omega t}\}. \tag{2.1}$$

and ω is the angular frequency of motion. Then ϕ_t satisfies

$$(\nabla^2 - l^2)\phi_t = 0, \quad -h < y < 0, \, -\infty < x < \infty, \tag{2.2}$$

$$\frac{\partial \phi_t}{\partial y} = 0, \quad y = -h, \, -\infty < x < \infty, \tag{2.3}$$

$$\mathcal{L}\phi_t \equiv \left(\beta \left(\frac{\partial^2}{\partial x^2} - l^2 \right)^2 + (1 - \delta) \right) \frac{\partial \phi_t}{\partial y} - \phi_t = 0, \quad y = 0, \, x \in (-\infty, 0) \cup (0, \infty). \tag{2.4}$$

Here, we have adopted the non-dimensionalisation and notation used by Tkacheva (2001a) in which lengths have been scaled by the frequency parameter $\kappa = \omega^2/g$ (g is acceleration due to gravity) and the wavenumber in the z-direction, l, has been scaled by $1/\kappa$. The dimensionless parameter β is defined by $\beta = D\kappa^4/(\rho_w g)$ where D is the flexural rigidity of the ice sheet and ρ_w is the density of the fluid. Also, the dimensionless quantity δ is defined to be $(\rho_i/\rho_w)d$ where ρ_i is the density, and d is the (non-dimensional) thickness, of the ice. To be consistent with the linearisation process, it is necessary in the problems considered by, for example, Evans & Davies (1968) and Tkacheva (2001a) which involve ocean waves interacting with floating ice sheets, to assume $d \ll 1$, implying $\delta \ll 1$, so that the condition (2.4) may be applied on $y = 0$ rather than $y = -d$. However, in the problem being considered here the entire surface is covered by ice of the same thickness so we may relax the smallness condition on δ and we therefore retain it throughout our analysis.

At the edges of the plates, we impose conditions of zero bending moment and zero shear stress, which are expressed by

$$\mathcal{B}\phi_t \equiv \left[\left(\frac{\partial^2}{\partial x^2} - \nu l^2 \right) \frac{\partial \phi_t}{\partial y} \right]_{y=0} \to 0, \quad \text{as } x \to 0^{\pm} \tag{2.5}$$

and

$$\mathcal{S}\phi_t \equiv \left[\frac{\partial}{\partial x} \left(\frac{\partial^2}{\partial x^2} - \nu_1 l^2 \right) \frac{\partial \phi_t}{\partial y} \right]_{y=0} \to 0, \quad \text{as } x \to 0^{\pm} \tag{2.6}$$

where $\nu_1 = 2 - \nu$ and ν is Poisson's ratio. Quantities of particular interest associated with the edges of the plate are then

$$P_t^{\pm} = \lim_{x \to 0^{\pm}} \left. \frac{\partial^2 \phi_t}{\partial x \partial y} \right|_{y=0} \quad \text{and} \quad Q_t^{\pm} = \lim_{x \to 0^{\pm}} \left. \frac{\partial \phi_t}{\partial y} \right|_{y=0} \tag{2.7}$$

which represent, respectively, the gradient and elevation at the edges of the semi-infinite plates on the positive and negative side of the crack at $x = 0$. Despite the vanishing of combinations of higher-order derivatives in (2.5) and (2.6) on the edges of the plates the quantities $P_t^{\pm}$ and $Q_t^{\pm}$ do not vanish.

In order to complete the description of the problem we must apply the appropriate radiation conditions at infinity. This is achieved by considering separable solutions of (2.2) subject to the conditions (2.3) and (2.4) in either regions $x > 0$ or $x < 0$. Such solutions are given by

$$\mathrm{e}^{\pm i k_n x} \, Y_n(y) \tag{2.8}$$

where $Y_n(y)$ satisfies

$$Y_n''(y) = \gamma_n^2 Y_n(y), \quad Y_n'(-h) = 0, \tag{2.9}$$

and

$$(\beta\gamma_n^4 + 1 - \delta)Y_n'(0) - Y_n(0) = 0 \tag{2.10}$$

in which we have defined

$$\gamma_n^2 = k_n^2 + l^2. \tag{2.11}$$

Equations (2.8), (2.9) and (2.10) constitute an eigensystem in which the eigenfunctions defined to be

$$Y_n(y) = \cosh\gamma_n(y+h) \tag{2.12}$$

are non-orthogonal. However it can be shown, by integrating by parts, that

$$\int_{-h}^{0} Y_n(y)Y_m(y)dy = C_n\delta_{nm} - \beta(\gamma_m^2 + \gamma_n^2)Y_m'(0)Y_n'(0) \tag{2.13}$$

(see, for example, Lawrie & Abrahams 2002) where

$$C_n = \tfrac{1}{2}\{h + (5\beta\gamma_n^4 + 1 - \delta)[Y_n'(0)/\gamma_n]^2\}. \tag{2.14}$$

Now substitution of equation (2.12) into (2.15) gives the dispersion relation

$$K(k_n) \equiv (\beta\gamma_n^4 + 1 - \delta)\gamma_n \tanh\gamma_n h - 1 = 0 \tag{2.15}$$

governing possible values of k_n. It can be shown that this has a pair of real roots $\pm\gamma_0$ with corresponding roots $\pm k_0$ which describe progressive waves, provided $\gamma_0 > l$. Note, however, that if $\gamma_0 < l$ no such waves are possible and any motion will be confined to the crack. For the time being we will consider only the case $\gamma_0 > l$ where waves are radiated by the crack. In addition there is a sequence of pure imaginary roots $\pm k_n$ with $n = 1, 2, \ldots$ and four complex roots $\pm k_{-1}$ and $\pm k_{-2}$ symmetric about the real and imaginary axes. Let the roots in the first and second quadrants be k_{-1} and k_{-2}.

Then we prescribe the far-field behaviour of ϕ_t by

$$\phi_t(x,y) \sim \begin{cases} \left(\mathrm{e}^{-ik_0x} + R_t\mathrm{e}^{ik_0x}\right)Y_0(y), & x \to \infty, \\ T_t\mathrm{e}^{-ik_0x}Y_0(y), & x \to -\infty \end{cases} \tag{2.16}$$

where R_t and T_t denote respectively the reflection and transmission coefficents due to a wave obliquely incident from $x = \infty$. If the crests of the incoming wave make an angle of θ with the crack along $x = y = 0$ then $l = k_0\tan\theta = \gamma_0\sin\theta$ and then clearly $\gamma_0 > l$.

Because of symmetry in the geometry of the problem about the plane $x = 0$ we can achieve considerable simplification by writing

$$\phi_t = \tfrac{1}{2}(\phi_{ts} + \phi_{ta}) \tag{2.17}$$

where ϕ_{ts} (ϕ_{ta}) is even (odd) about $x = 0$. Then we need only consider $x > 0$, using the fact that

$$\left.\begin{aligned} \phi_{ts}(-x,y) = \phi_{ts}(x,y) = \phi_t(x,y) + \phi_t(-x,y), \\ \phi_{ta}(-x,y) = -\phi_{ta}(x,y) = -\phi_t(x,y) + \phi_t(-x,y) \end{aligned}\right\}. \tag{2.18}$$

Since ϕ_t and $\partial\phi_t/\partial x$ are continuous functions throughout the fluid region then it follows that

$$\frac{\partial\phi_{ts}(0,y)}{\partial x} = \phi_{ta}(0,y) = 0, \quad -h < y < 0. \tag{2.19}$$

An important step in the solution procedure is to explicitly build the influence of the incident wave into ϕ_{ts} and ϕ_{ta} by writing, for $x \geq 0$

$$\left.\begin{aligned}\phi_{ts}(x,y) &= \phi_{0s}(x,y) + \phi_s(x,y)\\ \phi_{ta}(x,y) &= \phi_{0a}(x,y) + \phi_a(x,y)\end{aligned}\right\} \tag{2.20}$$

where $\phi_{0s}(x,y) = (\mathrm{e}^{-ik_0x} + \mathrm{e}^{ik_0x})Y_0(y)$ and $\phi_{0a}(x,y) = (\mathrm{e}^{-ik_0x} - \mathrm{e}^{ik_0x})Y_0(y)$ are respectively symmetric and anti-symmetric standing waves.

The functions $\phi_s(x,y)$ and $\phi_a(x,y)$ now describe *outgoing* waves only and if we write

$$\phi_{s,a}(x,y) \sim R_{s,a}\mathrm{e}^{ik_0x}Y_0(y), \quad x \to \infty \tag{2.21}$$

then it may be confirmed that

$$R_t = \tfrac{1}{2}(R_s + R_a), \quad \text{and} \quad T_t = 1 + \tfrac{1}{2}(R_s - R_a). \tag{2.22}$$

Applying Green's Identity to each of the functions ϕ_{ts}, ϕ_{ta} and ϕ_t in turn each with their complex conjugates and over the appropriate fluid region gives the usual energy balance relations, namely

$$|R_s + 1| = |R_a - 1| = 1, \quad |R_t|^2 + |T_t|^2 = 1. \tag{2.23}$$

Since the function ϕ_t has been decomposed into a pair of functions now defined in $x \geq 0$ only, all other properties relating to the problem need to be decomposed similarly. The principal difficulty here is associated with the limit of the quantity $\partial\phi_t/\partial y$ and its derivatives in x on $y = 0$ as $x \to 0^\pm$.

Clearly, (2.2)–(2.4) apply to the functions ϕ_s and ϕ_a separately. So consider first the boundary condition (2.5). Now $\mathcal{B}\phi_t$ is a continuous function of x which vanishes as $x \to 0^\pm$. Hence, from equation (2.18)

$$\mathcal{B}\phi_{ta} = \mathcal{B}\phi_{ts} = 0, \quad x = 0. \tag{2.24}$$

This also means that $\mathcal{B}\phi_a = 0$ at $x = 0$ and

$$(\mathcal{B}\phi_s)_{x=0} = -(\mathcal{B}\phi_{0s})_{x=0} = 2(k_0^2 + \nu l^2)Y_0'(0). \tag{2.25}$$

Similar arguments apply in the decomposition of ϕ_t under the operator $\mathcal{S}$ occurring in (2.6), the main difference being that $\mathcal{S}$ is a operator that is *odd* in x. Hence it can be shown in this case that

$$\mathcal{S}\phi_{ts} = \mathcal{S}\phi_s = 0, \quad x = 0 \tag{2.26}$$

and then that

$$(\mathcal{S}\phi_a)_{x=0} = -(\mathcal{S}\phi_{0a})_{x=0} = -2ik_0(k_0^2 + \nu_1 l^2)Y_0'(0). \tag{2.27}$$

Next, it is straightforward to confirm, using the definition of ϕ_t in (2.7), that

$$P_t^\pm = -ik_0Y_0'(0) + \tfrac{1}{2}(\pm P_s + P_a), \quad \text{and} \quad Q_t^\pm = Y_0'(0) + \tfrac{1}{2}(Q_s \pm Q_a) \tag{2.28}$$

where we define

$$P_{s,a} = \lim_{x\to 0} \left.\frac{\partial^2\phi_{s,a}}{\partial x\partial y}\right|_{y=0} \quad \text{and} \quad Q_{s,a} = \lim_{x\to 0} \left.\frac{\partial\phi_{s,a}}{\partial y}\right|_{y=0}. \tag{2.29}$$

In particular, the quantities

$$[P_t] \equiv P_t^+ - P_t^- = P_s, \quad \text{and} \quad [Q_t] \equiv Q_t^+ - Q_t^- = Q_a \tag{2.30}$$

depend upon just P_s and Q_a. As will be shown in the next section, these two quantities may be regarded as the fundamental unknowns in the problem since R_s and R_a may be determined from them directly.

3. Solution using a Green's function approach

We shall seek the solution to each of the symmetric and anti-symmetric problems in turn by using Green's Identity in conjunction with the appropriate Green's functions. Thus, we shall require Green's functions $G_s(x, y; \xi, \eta)$ and $G_a(x, y; \xi, \eta)$ defined for $x, \xi \geq 0$, $-h < y, \eta < 0$ which satisfy the conditions

$$\frac{\partial G_s(0, y; \xi, \eta)}{\partial x} = G_a(0, y; \xi, \eta) = 0, \quad -h < y < 0. \tag{3.1}$$

That is, G_s and G_a are symmetric and anti-symmetric (respectively) about $x = 0$. They may be written as the combinations

$$G_{s,a}(x, y; \xi, \eta) = G(x, y; \xi, \eta) \pm G(x, y; -\xi, \eta) \tag{3.2}$$

where subscripts $s(a)$ refer to upper (lower) signs respectively and $G(x, y; \xi, \eta)$ is the Green's function for the infinite strip $-\infty < x, \xi < \infty$ defined by

$$(\nabla^2 - l^2)G = \delta(x - \xi)\delta(y - \eta) \tag{3.3}$$

$$\frac{\partial G}{\partial y} = 0, \quad y = -h, \, -\infty < x < \infty \tag{3.4}$$

and

$$\mathcal{L}G = 0, \quad y = 0, \, -\infty < x < \infty \tag{3.5}$$

where $\mathcal{L}$ is defined by (2.4) and G is chosen to represent outgoing waves as $|x| \to \infty$. It is a standard procedure to derive the Green's function G by applying Fourier transform methods and details of its derivation are therefore not recorded here. We find that

$$G(x, y; \xi, \eta) = \frac{1}{2\pi} \int_{-\infty}^{\infty} \frac{\mathrm{e}^{-i\alpha|x-\xi|} f(\alpha, y_>, y_<)}{\gamma K(\alpha)} d\alpha \tag{3.6}$$

where

$$f(\alpha, y, \eta) = \cosh \gamma(\eta + h)\{-\sinh \gamma y - (\beta\gamma^4 + 1 - \delta)\gamma \cosh \gamma y\} \tag{3.7}$$

and $y_> = \max\{y, \eta\}$, $y_< = \min\{y, \eta\}$. Here,

$$K(\alpha) = (\beta\gamma^4 + 1 - \delta)\gamma \sinh \gamma h - \cosh \gamma h \tag{3.8}$$

where $\gamma^2 = \alpha^2 + l^2$ which coincides with the left-hand side of the dispersion relation (2.15) when $\alpha = \pm k_n$, $n = -2, -1, 0, 1, \ldots$. The path of integration in (3.6) passes above the pole of $K(\alpha)$ at $\alpha = -k_0$ and below the pole at $\alpha = k_0$ in order that the radiation condition be satisfied.

It is convenient for what follows to express G as an infinite series by deforming the path of integration in (3.6) downwards into the lower half-plane picking up contributions from the residues at the poles $\alpha = -k_n, n = -2, -1, 0, 1, 2...$ of the function $K(\alpha)$. Thus, making use of (3.2) we find, for $x, \xi \geq 0$,

$$G_{s,a}(x, y; \xi, \eta) = -i \sum_{n=-2}^{\infty} \frac{Y_n(y)Y_n(\eta)}{2k_n C_n} \{\mathrm{e}^{ik_n|x-\xi|} \pm \mathrm{e}^{ik_n(x+\xi)}\} \tag{3.9}$$

where the relation

$$K'(k_n) = -K'(-k_n) = 2k_n C_n / Y_n'(0) \tag{3.10}$$

has been used. In what follows we shall make use of

$$\left.\frac{\partial G_s}{\partial y}\right|_{y=0} = -i \sum_{n=-2}^{\infty} \frac{Y_n'(0)Y_n(\eta)}{k_n C_n} \cos k_n x \, \mathrm{e}^{ik_n\xi}, \quad \xi > x, \tag{3.11}$$

$$\left.\frac{\partial G_a}{\partial y}\right|_{y=0} = -\sum_{n=-2}^{\infty} \frac{Y_n'(0)Y_n(\eta)}{k_n C_n} \sin k_n x \, \mathrm{e}^{ik_n\xi}, \quad \xi > x. \tag{3.12}$$

It follows that, as expected, on $x = 0$

$$\left.\frac{\partial G_a}{\partial y}\right|_{y=0} = \left.\frac{\partial^3 G_a}{\partial x^2 \partial y}\right|_{y=0} = \left.\frac{\partial^2 G_s}{\partial x \partial y}\right|_{y=0} = \left.\frac{\partial^4 G_s}{\partial x^3 \partial y}\right|_{y=0} = 0 \tag{3.13}$$

since it can be shown, using methods similar to that described in the Appendix for related series, that all the corresponding infinite series are absolutely and uniformly convergent as $x \to 0$.

We shall also require

$$\mathcal{B}G_s \equiv \left[\left(\frac{\partial^2}{\partial x^2} - \nu l^2\right)\frac{\partial G_s}{\partial y}\right]_{y=0} \to i \sum_{n=-2}^{\infty} \frac{(\nu l^2 + k_n^2)Y_n'(0)}{k_n C_n} Y_n(\eta), \quad \text{as } x \to 0 \tag{3.14}$$

and

$$\mathcal{S}G_a \equiv \left[\frac{\partial}{\partial x}\left(\frac{\partial^2}{\partial x^2} - \nu_1 l^2\right)\frac{\partial G_a}{\partial y}\right]_{y=0} \to \sum_{n=-2}^{\infty} \frac{(\nu_1 l^2 + k_n^2)Y_n'(0)}{C_n} Y_n(\eta), \quad \text{as } x \to 0 \tag{3.15}$$

obtained from (3.11) and (3.12). Again it can be shown that both series are absolutely and uniformly convergent. We are now in a position to determine our solution. We only derive $\phi_s(x,y)$ in detail, stating the corresponding results for $\phi_a(x,y)$.

We apply Green's Identity to G_s and ϕ_s in the semi-infinite region $x > 0$, $-h < y < 0$, noting that since both functions describe outgoing waves to $x \to \infty$ there will only be a contribution to the integral around the boundary from the surface condition on $y = 0$. Thus, we have

$$\phi_s(\xi,\eta) = \int_0^{\infty} \left(\phi_s \frac{\partial G_s}{\partial y} - G_s \frac{\partial \phi_s}{\partial y}\right)_{y=0} dx. \tag{3.16}$$

The details of how we treat this integral are rather messy, but are of fundamental importance in the approach to this problem and will therefore be presented in some detail. Using the definition of the boundary operator on $y = 0$ we find

$$\begin{aligned}\phi_s(\xi,\eta) &= \int_0^{\infty} \left[\beta\left(\frac{\partial^2}{\partial x^2} - l^2\right)^2 \frac{\partial \phi_s}{\partial y}\frac{\partial G_s}{\partial y} - \beta\left(\frac{\partial^2}{\partial x^2} - l^2\right)^2 \frac{\partial G_s}{\partial y}\frac{\partial \phi_s}{\partial y}\right]_{y=0} dx \\ &= -2l^2\beta H + \beta\int_0^{\infty}\left[\frac{\partial^5 \phi_s}{\partial x^4 \partial y}\frac{\partial G_s}{\partial y} - \frac{\partial^5 G_s}{\partial x^4 \partial y}\frac{\partial \phi_s}{\partial y}\right]_{y=0} dx\end{aligned} \tag{3.17}$$

where

$$H = \int_0^{\infty}\left[\frac{\partial^3 \phi_s}{\partial x^2 \partial y}\frac{\partial G_s}{\partial y} - \frac{\partial^3 G_s}{\partial x^2 \partial y}\frac{\partial \phi_s}{\partial y}\right]_{y=0} dx. \tag{3.18}$$

Now applying integration by parts repeatedly to the second integral in (3.17) we obtain

$$\phi_s(\xi,\eta) = \beta(I - J - 2l^2 H) \tag{3.19}$$

where

$$I = \left[\frac{\partial^4 \phi_s}{\partial x^3 \partial y}\frac{\partial G_s}{\partial y} - \frac{\partial^4 G_s}{\partial x^3 \partial y}, \frac{\partial \phi_s}{\partial y}\right]_0^{\infty} \tag{3.20}$$

and

$$J = \left[\frac{\partial^3 \phi_s}{\partial x^2 \partial y}\frac{\partial^2 G_s}{\partial x \partial y} - \frac{\partial^3 G_s}{\partial x^2 \partial y}\frac{\partial^2 \phi_s}{\partial x \partial y}\right]_0^{\infty} \tag{3.21}$$

and both I and J are to be evaluated on $y=0$. Note that the integral remaining from twice integrating by parts vanishes.

Now we are able to make use of the boundary conditions at $x=y=0$. First, note from (2.6), (2.26)

$$\frac{\partial^4 \phi_s}{\partial x^3 \partial y} = \nu_1 l^2 \frac{\partial^2 \phi_s}{\partial x \partial y} = \nu_1 l^2 P_s \tag{3.22}$$

from the definition of P_s in (2.29). In conjunction with the results in (3.13) we find that

$$I = -\nu_1 l^2 P_s \left.\frac{\partial G_s}{\partial y}\right|_{x=y=0} \quad \text{and} \quad J = P_s \left.\frac{\partial^3 G_s}{\partial x^2 \partial y}\right|_{x=y=0}. \tag{3.23}$$

Note again, that all contributions from the limit $x=\infty$ in I and J vanish on account of both G_s and ϕ_s representing outgoing waves only as $x \to \infty$.

Finally, integration by parts in (3.18) gives

$$H = \left[\frac{\partial^2 \phi_s}{\partial x \partial y}\frac{\partial G_s}{\partial y} - \frac{\partial^2 G_s}{\partial x \partial y}\frac{\partial \phi_s}{\partial y}\right]_0^\infty = -P_s \left.\frac{\partial G_s}{\partial y}\right|_{x=y=0} \tag{3.24}$$

using (2.27) and (3.13). So now (3.19) is

$$\phi_s(\xi,\eta) = -\beta P_s \left[\left(\frac{\partial^2}{\partial x^2} - \nu l^2\right)\frac{\partial G_s}{\partial y}\right]_{x=y=0} = -\beta P_s (\mathcal{B}G_s)_{x=0} \tag{3.25}$$

where $\nu = 2-\nu_1$ has been used.

Substitution from (3.14) now gives after reverting to variables x, y,

$$\phi_s(x,y) = -i\beta P_s \sum_{n=-2}^{\infty} \frac{(\nu l^2 + k_n^2) Y_n'(0)}{k_n C_n} Y_n(y) \mathrm{e}^{ik_n x}. \tag{3.26}$$

Application of the boundary condition (2.25) now gives

$$2Y_0'(0)(k_0^2 + \nu l^2) = i\beta P_s \sum_{n=-2}^{\infty} \frac{(\nu l^2 + k_n^2)^2 [Y_n'(0)]^2}{k_n C_n} \tag{3.27}$$

and this equation determines P_s and hence $\phi_s(x,y)$ from (3.26). The convergence of the infinite sum is shown in the Appendix.

Notice that deriving P_s from (3.26) by using (2.29) results in an identity

$$\beta \sum_{n=-2}^{\infty} \frac{(\nu l^2 + k_n^2)[Y_n'(0)]^2}{C_n} = 1 \tag{3.28}$$

which is proved in the Appendix.

We next give brief details of how the method used above for the symmetric case goes through for the anti-symmetric case. This time, $\phi_a(x,y)$ is used in conjunction with Green's function $G_a(x,y;\xi,\eta)$ in Green's Identity. In this case, (2.24) and the properties of G_a in (3.13) are used to simplify various terms that arise during the integration by parts and eventually, it is found that

$$\phi_a(\xi,\eta) = \beta Q_a (\mathcal{S}G_a)_{x=0} \tag{3.29}$$

where $\mathcal{S}$ is defined by (2.6). Then, the analogue of (3.26) is

$$\phi_a(x,y) = \beta Q_a \sum_{n=-2}^{\infty} \frac{(\nu_1 l^2 + k_n^2) Y_n'(0)}{C_n} Y_n(y) \mathrm{e}^{ik_n x}. \tag{3.30}$$

Application of the remaining boundary condition (2.27) to ϕ_a gives

$$2iY_0'(0)k_0(k_0^2+\nu_1 l^2) = i\beta Q_a \sum_{n=-2}^{\infty} \frac{k_n(\nu_1 l^2+k_n^2)^2[Y_n'(0)]^2}{C_n} \tag{3.31}$$

which determines the value of Q_a.

Again, deriving Q_a from (3.30) using (2.29) results in an identity

$$\beta \sum_{n=-2}^{\infty} \frac{(\nu_1 l^2+k_n^2)[Y_n'(0)]^2}{C_n} = 1 \tag{3.32}$$

which is proved in the Appendix.

Taking the limit of $x \to \infty$ in either (3.26) or (3.30) picks out just the $n=0$ propagating wave mode from the infinite sum which, when compared with the assumed behaviour (2.21), reveals that

$$R_s = \left(\frac{-i\beta(k_0^2+\nu l^2)Y_0'(0)}{k_0 C_0} \right) P_s \tag{3.33}$$

and

$$R_a = \left(\frac{\beta(k_0^2+\nu_1 l^2)Y_0'(0)}{C_0} \right) Q_a. \tag{3.34}$$

Hence, it is only necessary to calculate the quantities P_s and Q_a in order to determine the reflection and transmission coefficients, as predicted at the end of section 2.

The relations (3.33) and (3.34) may be derived independently without having to derive the complete solution by applying Green's Identity to the two functions ϕ_s and ϕ_{0s} in the former case and to ϕ_a and ϕ_{0a} in the latter case in the region $0<x<\infty$ and $-h<y<0$. This process uses properties of the various functions at the point $x=0$ and for large x and has many similarities with the application of Green's Identity already detailed in this section.

4. Solution using an eigenfunction expansion method

The infinite series for ϕ_s and ϕ_a obtained in the previous section were sums over all roots of the dispersion relation (2.15) suggesting that such an expansion is complete. In this section we show that adopting such an eigenfunction expansion from the outset and applying all the conditions required for the solution of the symmetric and anti-symmetric parts of the problem leads to the same solution as found in the previous section with much less effort. The same approach has been used by Lawrie & Abrahams (1999) in a related membrane problem, and also in determining the possible modes in a semi-infinite rectangular duct bounded by three rigid walls and an elastic plate (Lawrie & Abrahams 2002).

Consider the problem for $\phi_s(x,y)$ defined in $x \geq 0$ found in the previous section and let us assume an expansion in terms of the separable solutions in (2.8) ensuring that the solution at infinity remains bounded. That is, we write

$$\phi_s(x,y) = \sum_{n=-2}^{\infty} A_n \mathrm{e}^{ik_n x} Y_n(y) \tag{4.1}$$

where the $Y_n(y)$ are non-orthogonal functions over $[-h,0]$ which satisfy the relation

(2.13), which is reproduced here for convenience:

$$\int_{-h}^{0} Y_n(y)Y_m(y)dy = C_n\delta_{nm} - \beta(\gamma_m^2 + \gamma_n^2)Y_m'(0)Y_n'(0). \tag{4.2}$$

Application of the condition (2.19) gives

$$0 = \sum_{n=-2}^{\infty} ik_n A_n Y_n(y) \tag{4.3}$$

and then multiplying by $Y_m(y)$ and integrating over $-h < y < 0$ using (4.2) now gives

$$k_m A_m C_m = \beta\gamma_m^2 Y_m'(0) \sum_{n=-2}^{\infty} k_n A_n Y_n'(0) + \beta Y_m'(0) \sum_{n=-2}^{\infty} \gamma_n^2 k_n A_n Y_n'(0). \tag{4.4}$$

Applying (2.26) with $\mathcal{S}$ defined by (2.6) to (4.1) gives the identity

$$0 = \sum_{n=-2}^{\infty} k_n(k_n^2 + \nu_1 l^2)A_n Y_n'(0) \tag{4.5}$$

which may be expressed, using the relation $\gamma_n^2 = k_n^2 + l^2$, as

$$\sum_{n=-2}^{\infty} k_n\gamma_n^2 A_n Y_n'(0) = (1-\nu_1)l^2 \sum_{n=-2}^{\infty} k_n A_n Y_n'(0). \tag{4.6}$$

It can be seen from (2.29) and (4.1) that the summation on the right-hand side of (4.6) is simply $-iP_s$ and so using (4.6) in (4.4) we have

$$k_m A_m C_m = -i\beta\gamma_m^2 Y_m'(0)P_s - i\beta(1-\nu_1)l^2 Y_m'(0)P_s = -i\beta P_s(k_m^2 + \nu l^2)Y_m'(0) \tag{4.7}$$

since $\nu_1 = 2 - \nu$. Putting (4.7) into (4.1) results in (3.26) with P_s determined, as before, by applying (2.25) to obtain (3.27).

A similar approach to the solution of the antisymmetric problem for $\phi_a(x, y)$ results in the series (3.30). Thus we seek a solution

$$\phi_a(x, y) = \sum_{n=-2}^{\infty} B_n \mathrm{e}^{ik_n x} Y_n(y). \tag{4.8}$$

In this case the Dirichlet condition satisfied by ϕ_a gives

$$0 = \sum_{n=-2}^{\infty} B_n Y_n(y). \tag{4.9}$$

Again we multiply by $Y_m(y)$ and integrate over $-h < y < 0$ using the non-orthogonal condition (4.2) to obtain

$$B_m C_m = \beta\gamma_m^2 Y_m'(0) \sum_{n=-2}^{\infty} B_n Y_n'(0) + \beta Y_m'(0) \sum_{n=-2}^{\infty} \gamma_n^2 B_n Y_n'(0). \tag{4.10}$$

In this case the required condition to be satisfied at the plate edge by ϕ_a is that given above (2.25) with $\mathcal{S}$ defined by (2.5) which produces the identity

$$0 = \sum_{n=-2}^{\infty} (k_n^2 + \nu l^2)B_n Y_n'(0) \tag{4.11}$$

and this may be written

$$\sum_{n=-2}^{\infty} \gamma_n^2 B_n Y_n'(0) = (1-\nu)l^2 \sum_{n=-2}^{\infty} B_n Y_n'(0). \tag{4.12}$$

We now substitute (4.12) into (4.10) noting from (2.29) and (4.8) that the sum on the right-hand side of (4.12) is Q_a to obtain

$$B_m C_m = \beta\gamma_m^2 Y_m'(0) Q_a + \beta(1-\nu)l^2 Y_m'(0) Q_a = \beta Q_a (k_m^2 + \nu_1 l^2) Y_m'(0). \tag{4.13}$$

If we now substitute (4.13) into (4.8) we obtain the expression (3.30) with Q_a determined, as before, by applying (2.27) to obtain (3.31).

5. Edge waves along the crack

From (2.15) to (2.12) it is clear that for a given γ_0 corresponding to a root k_0 of the dispersion relation, we can increase the angle θ which the incident wave crests make with the crack, and hence the component of the wavenumber l in the direction of the crack, since $l = \gamma_0 \sin\theta$, until θ approaches $\pi/2$ and the direction of the incident wave is almost parallel to the crack. For values of $l > \gamma_0$, however, no progressive wave is possible and this defines a cut-off frequency, $\omega_c(l)$ say, which may be determined from the dispersion relation (2.15) by taking $\gamma_0 = l$. That is, $\omega_c(l)$ may determined from $(\beta l^4 + 1 - \delta) l \sinh lh = \cosh lh$ where, due to the non-dimensionalisation employed, the frequency is embedded in the three terms β, δ and h. Then for a given wavenumber component in the direction of the crack, l, and wave frequency ω less than the cut-off value of $\omega_c(l)$, no wave can be incident from infinity and no wave can radiate from the crack away to infinity. Thus, there is the possibility of generating edge waves, trapped along the length of the crack which decay exponentially away from the crack. Since there is no incident wave a solution can be sought which is either symmetric or antisymmetric about $x = 0$ and each part can be constructed as before, bearing in mind that throughout $\gamma_0 < l$. The only major difference comes when applying the final condition of the problem in each case. Previously, the presence of the incident wave provides an inhomogeneous equation defining the values of P_s and Q_a, namely (3.27) and (3.31). In the edge wave case, where $\gamma_0 < l$ the left-hand sides of these equations vanish (since the problem is homogeneous and the values of P_s and Q_a can be chosen arbitrarily) and one is left with the conditions

$$i \sum_{n=-2}^{\infty} \frac{(\nu l^2 + k_n^2)^2 [Y_n'(0)]^2}{k_n C_n} = 0 \tag{5.1}$$

for symmetric edge waves and

$$i \sum_{n=-2}^{\infty} \frac{k_n (\nu_1 l^2 + k_n^2)^2 [Y_n'(0)]^2}{C_n} = 0 \tag{5.2}$$

for antisymmetric edge waves.

Since $\gamma_0 < l$, k_0 now lies on the imaginary axis along with the roots k_n, $n = 1, 2, \ldots$. Using the fact that $k_{-2} = -\overline{k_{-1}}$, where the overbar denotes complex conjugate, it is not difficult to show that the left-hand sides of both (5.1) and (5.2) are real. Hence, as is common in problems where trapped waves are to be determined, the conditions to be satisfied are real.

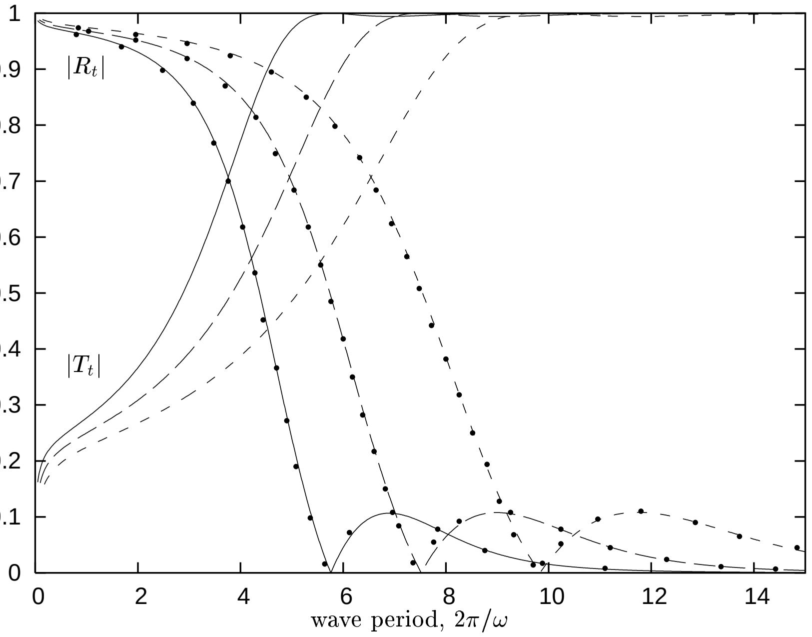

FIGURE 1. Variation of reflection and transmission coefficients with wave period for the configuration considered by Squire and Dixon (2000) with ice thicknesses, $\bar{d}$ of 0.5m (solid), 1m (long dashed) and 2m (short dashed) in water of depth $\bar{h}/\bar{d} = 80$. See text for other parameters.

6. Results

The governing equations in (2.1)–(2.6) have been presented in a dimensionless form which was chosen to reduce the complexity of the mathematical formulation. They were derived from the dimensional equations (see Fox & Squire (1994) for example) by scaling lengths with a frequency parameter, $\kappa = \omega^2/g$ and wavenumbers by $1/\kappa$. For the purpose of presenting meaningful results we shall re-introduce physical variables and also spend a little time identifying various important non-dimensional quantities that arise from this. The system that we shall employ is as follows: all physical lengths and wavenumbers shall be denoted by barred symbols. Accordingly, the actual depth of the fluid is $\bar{h}$ where $h = \kappa\bar{h}$ whilst $d = \kappa\bar{d}$ and the actual wavenumbers $\bar{l}$ and $\bar{\gamma}_0$ which are defined in terms of dimensionless wavenumbers l and γ_0 by $\bar{l} = \kappa l$ and $\bar{\gamma}_0 = \kappa\gamma_0$.

We choose to write the non-dimensional parameter β introduced in (2.4) as $\beta'(\kappa\bar{d})^4$ where $\bar{d}$ is the physical thickness of the sheet and now $\beta' = D/(\rho_w g\bar{d}^4)$ is a non-dimensional parameter which depends only on properties relating to the plate and the fluid it rests on. In terms of other physical constants, D is given by $E\bar{d}^3/(12(1-\nu^2))$ where E is Young's modulus and ν is Poisson's ratio. Squire & Dixon (2000) provide values for the various physical constants which occur in the definition of β' corresponding to an ice sheet on water which we shall adopt here. They define values of $E = 5$GPa, $\nu = 0.3$, $\rho_w = 1025\,\mathrm{kg\,m^{-3}}$ which gives a value of $\beta' = 45536/\bar{d}$, $\bar{d}$ being the thickness of the plate. In a similar manner, we separate frequency from δ by writing $\delta = \delta'(\kappa\bar{d})$ where $\delta' = \rho_i/\rho_w$ and $\rho_i = 922.5\,\mathrm{kg\,m^{-3}}$ is the density of ice so that $\delta' = 0.9$ is a fixed constant.

A further non-dimensional parameter that we use is $\bar{h}/\bar{d}$ which indicates the depth of water with respect to the thickness of the ice sheet.

We use a variety of different measures to characterise the wave motion on the sheets.

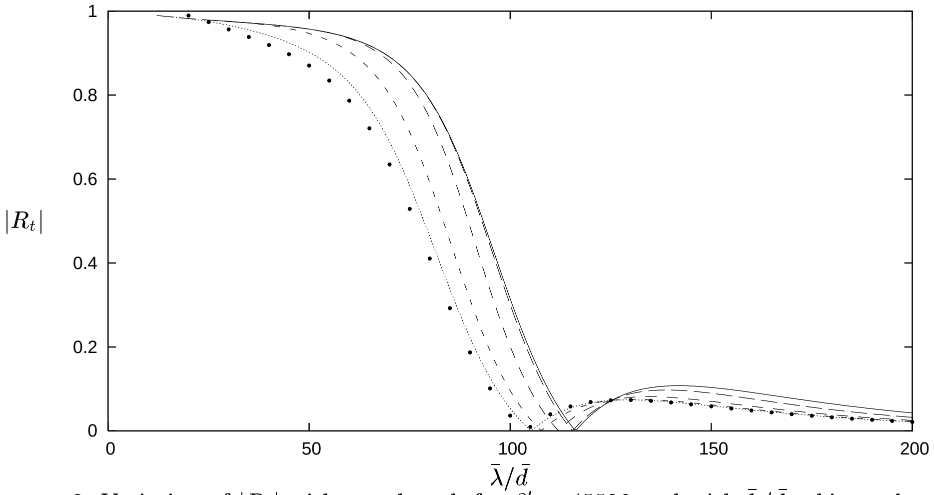

FIGURE 2. Variation of $|R_t|$ with wavelength for $\beta' = 45536$ and with $\bar{h}/\bar{d}$ taking values of 80 (solid), 40 (long dashed), 20 (medium dashed), 10 (short dashed) and 5 (dotted). Points are for shallow water theory for $\bar{h}/\bar{d} = 5$.

Perhaps the most useful is $\bar{\lambda}/\bar{d}$, where $\bar{\lambda} = 2\pi/\bar{\gamma}_0$ is the wavelength of the obliquely-incident wave. In terms of quantities appearing throughout our formulation we have $\bar{\lambda}/\bar{d} = (2\pi\bar{h}/\bar{d})/(\gamma_0 h)$ since $\gamma_0 h = \bar{\gamma}_0\bar{h}$.

To summarise then, in order to determine the solution we need to provide values of β', δ' and $\bar{h}/\bar{d}$, $\bar{\lambda}/\bar{d}$ which together combine to give $\gamma_0 h$ and θ, the angle of incidence. Once these are known, the dispersion relation (2.15), which may now be written as

$$(\beta''(\gamma_0 h)^4 + 1 - \delta'' h)(\gamma_0 h)\tanh(\gamma_0 h) - h = 0$$

where $\beta'' = \beta'(\bar{h}/\bar{d})^{-4}$, $\delta'' = \delta'(\bar{h}/\bar{d})^{-1}$ determines $h = \kappa\bar{h}$ and hence the frequency. Having found h we can go back to the dispersion relation in its original dimensionless form (2.15) and determine the roots γ_n, $n = -2, -1, 1, 2, \ldots$ and hence all other quantities needed to compute the solution.

In order to compare our results with those of Squire & Dixon (2000) we measure the variation of $|R_t|$ and $|T_t|$ with wave period $(2\pi/\omega)$ and choose $\bar{h}/\bar{d} = 80$, large enough to be considered as water of infinite depth. In figure 1 we show curves of $|R_t|$ and $|T_t|$ for ice thickness $\bar{d}$ of 0.5m, 1m and 2m and add to the curves of $|R_t|$ points taken from figure 2 of Squire & Dixon (2000) which clearly confirm the accuracy of our solution.

We should, at this point, mention the accuracy of the numerical scheme. Due to the high rate of convergence of the series that are computed (see the Appendix), very few terms are needed in the evaluation of the infinite sums which arise. For the results computed here the infinite sums were truncated at the 100th term, more than enough to ensure accuracy to six decimal places in all cases. The pure real root and sequence of pure imaginary roots of the dispersion relation (2.15) are not difficult to find numerically. For the pair of complex roots, only the root in the first quadrant needs to be found since the other is expressible in terms of it. For this, we use a fixed point algorithm suggested by Fox & Chung (1998).

In figure 2 we present the variation of $|R_t|$ with wavelength $\bar{\lambda}/\bar{d}$ for $\beta' = 45536$ (equivalent to $\bar{d} = 1$m in figure 1) in water of different depths. There is little overall change in the reflection due to the varying depth of the fluid, as may be expected. The solid curve in figure 2 corresponds to a depth to plate thickness ratio of $\bar{h}/\bar{d} = 80$, and the sequence

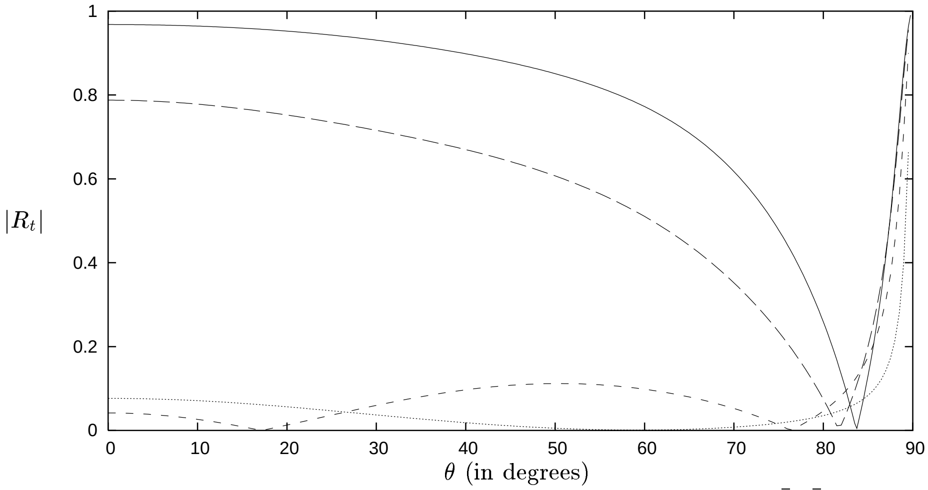

FIGURE 3. Variation of $|R_t|$ with angle of incidence, θ, for $\beta' = 45536$, $\bar{h}/\bar{d} = 40$ and for wavelengths $\bar{\lambda}/\bar{d}$ of 40 (solid), 80 (long dashed), 120 (short dashed) and 160 (dotted).

of curves that shift away to the left of this solid curve represent values of $\bar{h}/\bar{d}$ equal to 40, 20, 10 and 5. The set of points overlaid onto figure 2 are computed using a shallow-water approximation for $\bar{h}/\bar{d} = 5$ which compares favourably with the corresponding curve based on the full linear solution. This approximation, valid on the assumption that $\bar{\lambda}/\bar{d} \gg 1$ can be obtained by making a shallow-water approximation to the original boundary-value for ϕ_t in (2.1)–(2.6). Alternatively, the same result can be obtained by letting $h \to 0$ in the solution to the full linear problem has the effect of reducing the dispersion relation (2.15) to

$$(\beta\gamma_n^4 + 1 - \delta)\gamma_n^2 h - 1 = 0,$$

a cubic in γ_n^2 which has two real roots $\pm\gamma_0$ and two pairs of complex roots labelled $\pm\gamma_{-1}$ and $\pm\gamma_{-2}$ where $\gamma_{-1} = -\overline{\gamma_{-2}}$. The corresponding solutions for ϕ_s and ϕ_a are given by (3.26) and (3.30) where the infinite sum is reduced to a sum over $n = -2, -1, 0$. Similarly, the equations (3.27) and (3.31) defining P_s and Q_a also have the infinite sums replaced by sums over $n = -2, -1, 0$.

The effect of incident wave angle upon the reflection coefficient is presented for a typical case ($\beta' = 45536$, $\bar{h}/\bar{d} = 40$, $\nu = 0.3$) in figure 3 for four different wavelengths of $\bar{\lambda}/\bar{d} = 40$, 80, 120 and 160. In all cases, as the incident wave approaches a grazing angle with the crack, the reflection coefficient rises sharply to a value of unity in modulus. For relatively short wavelengths, there is a large reflection coefficient for most wave angles although the reflection coefficient dips to zero as θ approaches $\pi/2$ before shooting back up to unity. A similar type of behaviour is seen for the longer wavelength of $\bar{\lambda}/\bar{d} = 80$ whereas for $\bar{\lambda}/\bar{d} = 120$ there are two incident angles at which R_t is zero. Beyond this wavelength, the reflection coefficient tends to zero over most incident angles.

To give an impression of what the wave field actually looks like we plot, in figure 4, a snapshot in time of the surface displacement, defined by $\partial\phi_t/\partial y|_{y=0}$, of the ice sheets either side of the crack when a wave of wavelength $\bar{\lambda}/\bar{d} = 100$ is incident at an angle of $\theta = 30°$ on the crack. In this case, the wave is partially reflected by the crack which gives rise to a standing-wave pattern to the right of the figure and partially transmitted beyond the crack where the wave field rapidly develops into a progressing wave only as

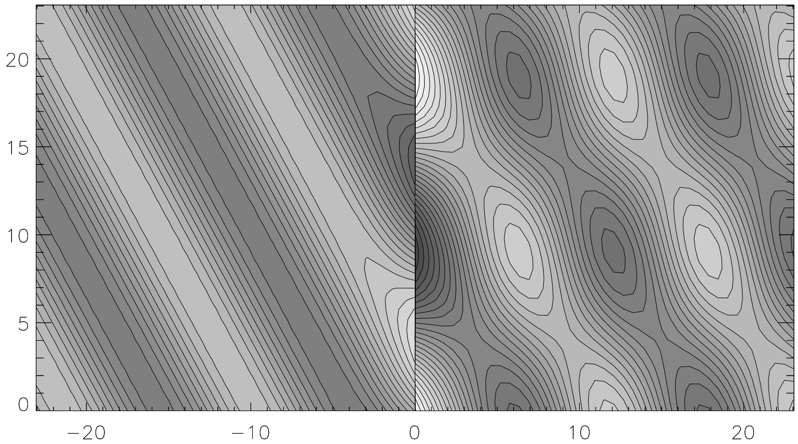

FIGURE 4. A snapshot of surface displacement $\partial\phi_t/\partial y|_{y=0}$ either side of a crack for a wave incident from the right with $\bar{\lambda}/\bar{d} = 100$ and $\theta = 30°$. Here $\beta' = 45536$, $\bar{h}/\bar{d} = 40$. Shading from light to dark represents the displacement from peaks to troughs.

the distance from the crack increases. The discontinuity in displacement and gradient across the crack is clearly visible from the figure.

In all the results for scattering of waves by a crack, physical constants corresponding to ice sheets floating on water have been used. In particular we have used the value of $\nu = 0.3$ for Poisson's ratio. In seeking edge wave solutions, it turns out to be of interest to consider larger values of ν. This is because, when using a value of $\nu = 0.3$, edge waves only occur at values of wave frequency extremely close to the cut-off frequency referred to in section 5. So let us first consider possible edge wave solutions, given by the satisfaction of the conditions (5.1) for symmetric edge waves and (5.2) for antisymmetric edge waves in the case $\gamma_0 < l$, as discussed in section 5. In figure 5 curves are shown for values of $\nu = 0.9$ reducing to $\nu = 0.6$ for $\beta' = 10^4$ and $\bar{h}/\bar{d} = 10$ so that the combination $\beta'' = \beta'(\bar{h}/\bar{d})^{-4}$ is equal to unity. This choice is made to conform with the only numerical results known to the authors on edge waves along cracks in ice sheets given by Marchenko (1999). However, Marchenko's equations were presented in a very different dimensional form, he was working in water of infinite depth and he made the unrealistic choice of $\nu = 1$ so no direct comparison with his results is attempted here. In figure 5 we have plotted curves showing the variation of non-dimensional wave frequency $\omega\sqrt{\bar{d}/g}$ with non-dimensional wavenumber in the direction of the crack, $\bar{l}\bar{d}$ for which edge waves exist. Also displayed in figure 5 is the heavy curve showing the cut-off frequency, $\omega_c(\bar{l}\bar{d})$ above which waves may be radiated to infinity and below which edge waves may exist. This curve is defined by the dispersion relation when $\gamma_0 = l$ (as already discussed in section 5) and may be written in the form

$$\omega_c(\bar{d}/g)^{1/2} = \left(\frac{(\beta'(\bar{l}\bar{d})^4 + 1)\bar{l}\bar{d}}{\delta'\bar{l}\bar{d} + \coth(\bar{l}\,\bar{h})}\right)^{1/2}.$$

It can be seen from figure 5 that as ν is reduced the curves of ω against $\bar{l}\bar{d}$ rapidly approach the cut-off frequency ω_c. All these curves are for symmetric edge waves; it appears that no antisymmetric edge waves exist for $\nu < 1$ as also noted by Marchenko (1999).

Edge waves do exist for $\nu = 0.3$ corresponding to ice, and a selection of edge wave parameters are presented in table 1 for ice of different thickness, $\bar{d}$. However, in all cases

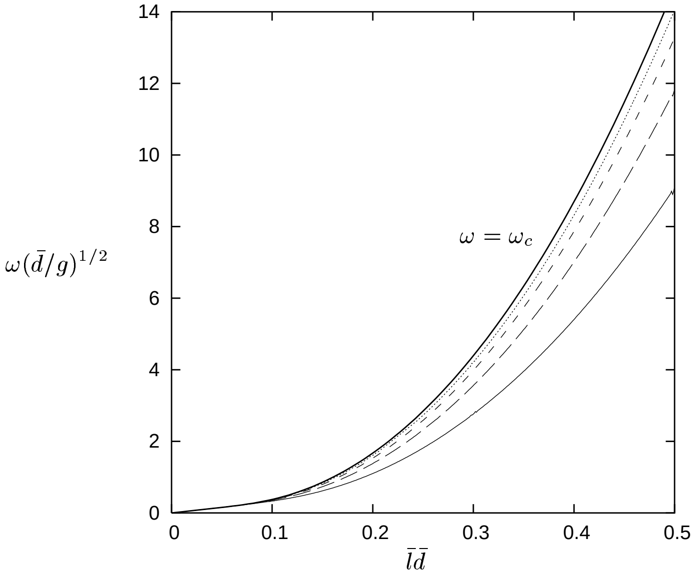

FIGURE 5. Variation of non-dimensional wave frequency $\omega(\bar{d}/g)^{1/2}$ with non-dimensional wavenumber $\bar{l}\bar{d}$ for edge waves along the crack between two plates with $\beta' = 10000$, $\bar{h}/\bar{d} = 10$ and with $\nu = 0.9$ (solid), 0.8 (long dashed), 0.7 (short dashed), 0.6 (dotted).

		$\beta' = 4553$	$\beta' = 45536$	$\beta' = 455360$
$\bar{l}\bar{d}$	$\omega_c(\bar{d}/g)^{1/2}$		$\omega(\bar{d}/g)^{1/2}$	
0.04	0.123910	0.123873	0.123904	-
0.08	0.266655	0.266650	0.266490	0.266618
0.12	0.528693	0.528687	0.528358	0.528296
0.16	0.985268	-	-	0.984114
0.20	1.657675	-	-	1.655698
0.24	2.554927	-	-	2.554674

TABLE 1. Values of frequency at which symmetric edge waves occur for ice sheets of thickness $\bar{d} = 10$m $\bar{d} = 1$m and $\bar{d} = 0.1$m for various values of $\bar{l}\bar{d}$. Here, $\nu = 0.3$, $\beta' = 45536$ and $\bar{h}/\bar{d} = 40$.

the wave frequency at which the edge wave occurs is very close to the cut-off. The two left-hand columns in table 1 show values of $\bar{l}\bar{d}$ and the corresponding cut-off frequency $\omega_c(\bar{d}/g)^{1/2}$. The remaining columns show values of $\omega(\bar{d}/g)^{1/2}$ in the three different cases considered which correspond to, in the case of ice sheets, thicknesses of $\bar{d} = 10$m $\bar{d} = 1$m and $\bar{d} = 0.1$m reading columns from left to right. In all three cases we have taken $\bar{h}/\bar{d} = 40$ since the results do not vary much with the depth of the water. Where there is no value displayed, it indicates that the edge wave is so close to the cut-off that there is no difference between the computed values of ω and ω_c in the sixth decimal place.

Finally, we illustrate in figure 6 the displacement of just one half of a symmetric edge wave propagating along the crack in a realistic case of $\nu = 0.3$, $\beta' = 45536$ (corresponding to an ice thickness of $\bar{d} = 1$m), $\bar{h}/\bar{d} = 10$ To generate this edge wave we have chosen $\bar{l}\bar{d} = 0.12$ (corresponding to a wavelength along the crack of $\bar{\lambda}/\bar{d} \simeq 50$) which gives a value of $\bar{\gamma}_0\bar{d} = 0.11995$, very close to the cut-off. The vertical scaling in figure 6 is arbitrary and

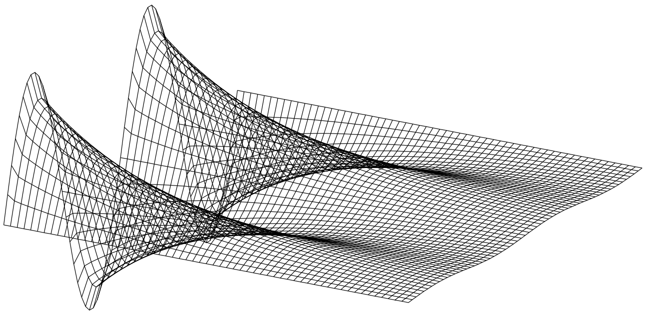

FIGURE 6. Snapshot in time of the displacement of one ice sheet for an edge wave with $\beta' = 45536$, $\nu = 0.3$ $\bar{h}/\bar{d} = 10$, $\bar{l}\bar{d} = 0.12$ and $\bar{\gamma}_0\bar{d} = 0.11995$. The edge wave is symmetric, there are two wavelengths in the z-direction and the figure is scaled to show 20 wavelengths in the x-direction.

scaling in the x-direction (away from the crack) represents a distance twenty times the wavelength along the crack. In this case, since the edge wave is so close to the cut-off it decays very slowly away from the crack. In other cases involving larger values of ν where edge waves can be generated further away from the cut-off the waves decay much more rapidly with distance from the crack.

7. Conclusion

In this paper an explicit solution has been obtained for the scattering of an obliquely-incident wave by a narrow line crack separating two semi-infinite elastic half-planes floating on water of finite depth. Previous approaches to the problem have regarded it as a special case of a Wiener-Hopf problem in which the boundary conditions on each half-plane are the same. This results in an unwieldy solution involving four constants which need to be determined from the edge conditions at each plate. Our approach has followed that of Squire and Dixon (2000) who use an appropriate Green's function in deep water and Green's identity to construct the solution. They build in the continuity of bending moment and shearing stress at the edges, in terms of what are in effect the constants P_s and Q_a defined here, which are then determined by applying the vanishing of the bending moment and shearing stress. Our approach has been to exploit the symmetry of the problem, solving two separate problems for the symmetric and anti-symmetric parts. Whilst being restrictive in application, this provides considerable simplification since working in $x > 0$ means that both potentials and Green's functions behave the same for large x so that there is no contribution from large x, and also the symmetry ensures that only one of the edge conditions needs to be applied to each part.

Having derived the solution, an alternative simple eigenfunction expansion method is described which, from the Green's theorem approach, could now be assured to be complete despite the non-standard nature of the problem with the eigenfunctions being non-orthogonal. In what may have otherwise appeared fortuitous in the eigenfunction expansion method, the Green's function approach shows, via the various symmetry properties of the functions employed, exactly how certain summations reduce to the constant P_s only in the symmetric problem and Q_a only in the antisymmetric problem.

Throughout the paper considerable care has been taken over convergence matters which plague such high-order boundary-value problems. Results have been presented for the variation of reflection and transmission coefficients with incident wavelength and angle of incidence and plate properties. For normally-incident waves and large depths our results appear to be in total agreement with Squire and Dixon (2000).

Finally the consideration of obliquely-incident waves has demonstrated the existence of localised edge waves travelling symmetrically along the crack in the absence of incident waves. For realistic values of Poisson's ratio ν, these occur extremely close to the cut-off frequency $\omega = \omega_c$ and only by varying ν up to values close to unity is there any appreciable variation of ω from ω_c. Similar results have been obtained by Marchenko (1999) for deep water where ν was taken to be unity. It ought to be possible to obtain a wider range of edge waves for the case of ice by considering a crack of finite width. This problem, and the corresponding scattering problem will form the basis of a future paper by the authors.

Appendix

Throughout the paper various infinite series are derived, all of which can be shown to be absolutely and, where appropriate, uniformly convergent. Typical of these is the sum

$$S_m = \sum_{n=-2}^{\infty} \frac{k_n^m [Y_n'(0)]^2}{C_n} \tag{A.1}$$

for $m \geq 0$ where $Y_n(y)$ and C_n are defined by (2.12) and (2.14), and k_n are the roots of (2.15). Now $k_n \sim in\pi$, as $n \to \infty$ and so $\gamma_n = (k_n^2 + l^2)^{\frac{1}{2}} \sim in\pi$, $n \to \infty$ also.

We have

$$\begin{aligned} S_m &= \sum_{n=-2}^{\infty} \frac{2k_n^m \gamma_n^2 \sinh^2(\gamma_n h)}{h + \sinh^2(\gamma_n h)(5\beta\gamma_n^4 + 1 - \delta)} \\ &= \sum_{n=-2}^{\infty} \frac{2k_n^m \gamma_n^2 \tanh^2(\gamma_n h)}{h + \tanh^2(\gamma_n h)(5\beta\gamma_n^4 + 1 - \delta - h)} \end{aligned} \tag{A.2}$$

and since from (2.15) $\tanh \gamma_n h = 1/(\gamma_n(\beta\gamma_n^4 + 1 - \delta))$ we find

$$S_m = \sum_{n=-2}^{\infty} a_n k_n^m, \quad a_n = \frac{2\gamma_n^2}{((5\beta\gamma_n^4 + 1 - \delta - h) + h\gamma_n^2(\beta\gamma_n^4 + 1 - \delta)^2)} \tag{A.3}$$

and $a_n = O(1/n^8)$ as $n \to \infty$. So the series S_m is absolutely convergent for $m \leq 6$.

This shows in particular that the series in the definitions of P_s from (3.27) and Q_a from (3.31) are absolutely convergent, and a minor extension of the previous argument is sufficient to show that the series (3.26) and (3.30) defining ϕ_s and ϕ_a are absolutely and uniformly convergent.

In the course of the paper the identities (3.28) and (3.32) were derived which together imply

$$\sum_{n=-2}^{\infty} \frac{[Y_n'(0)]^2}{C_n} = 0 \tag{A.4}$$

and

$$\sum_{n=-2}^{\infty} \frac{k_n^2 [Y_n'(0)]^2}{C_n} = \beta^{-1}. \tag{A.5}$$

Also, in section 2, the continuity of $\mathcal{S}\phi_t$ from (2.6) at $x = 0$ enabled us to assert, in

(2.26) that $\mathcal{S}\phi_s = 0$ at $x = 0$. This would imply, from (3.26) that

$$\sum_{n=-2}^{\infty} \frac{(\nu l^2 + k_n^2)(\nu_1 l^2 + k_n^2)[Y_n'(0)]^2}{C_n} = 0 \tag{A.6}$$

which is consistent with (A.4) and (A.5) if

$$\sum_{n=-2}^{\infty} \frac{k_n^4 [Y_n'(0)]^2}{C_n} = -2l^2\beta^{-1} \tag{A.7}$$

since $\nu + \nu_1 = 2$.

Satisfaction of (A.6) also shows that $\mathcal{B}\phi_a = 0$ at $x = 0$ as asserted after (2.24) as a result of the continuity of $\mathcal{B}\phi_t = 0$ from (2.5).

We now prove the identities (A.4), (A.5) and (A.7). First note that all three series are absolutely convergent.

Now

$$\sum_{n=-2}^{\infty} \frac{[Y_n'(0)]^2}{C_n} = 2\sum_{n=-2}^{\infty} \frac{k_n \gamma_n \sinh \gamma_n h}{K'(k_n)}$$

from (3.10).

Consider the integral

$$I_1 = \frac{1}{2\pi i} \oint \frac{\alpha\gamma \sinh \gamma h}{K(\alpha)} d\alpha$$

where the contour is a circle, centre the origin of radius R.

The integrand is $O(\alpha^{-3})$ on R as $R \to \infty$ so that $I_1 \to 0$ as $R \to \infty$. Also, since the integrand is odd in α, the contributions from the poles of $K(\alpha)$ at $\alpha = k_n$ double up with those from $\alpha = -k_n$ and we find that

$$I_1 = \sum_{n=-2}^{\infty} \frac{k_n \gamma_n \sinh \gamma_n h}{K'(k_n)} = 0$$

which proves (A.4).

Next consider

$$I_2 = \frac{1}{2\pi i} \oint \left(\frac{\beta\alpha^3 \gamma \sinh \gamma h}{K(\alpha)} - \frac{1}{\alpha} \right) d\alpha.$$

Again the integrand is $O(\alpha^{-3})$ on R as $R \to \infty$ and is odd, so that

$$I_2 = 2\sum_{n=-2}^{\infty} \frac{\beta k_n^3 \gamma_n \sinh \gamma_n h}{K'(k_n)} - 1 = \beta \sum_{n=-2}^{\infty} \frac{k_n^2 [Y_n'(0)]^2}{C_n} - 1 = 0$$

and (A.5) is proved.

Finally consider

$$I_3 = \frac{1}{2\pi i} \oint \left(\frac{\beta\alpha^5 \gamma \sinh \gamma h}{K(\alpha)} - \alpha + \frac{2l^2}{\alpha} \right) d\alpha$$

where once more the integrand is $O(\alpha^{-3})$ on R as $R \to \infty$ and is odd in α. Thus, as before,

$$I_3 = 2\sum_{n=-2}^{\infty} \frac{\beta k_n^5 \gamma_n \sinh \gamma_n h}{K'(k_n)} + 2l^2 = \beta \sum_{n=-2}^{\infty} \frac{k_n^4 [Y_n'(0)]^2}{C_n} + 2l^2 = 0$$

and (A.7) is proved. The conditions (2.19) are applied both in the course of the Green's function construction of the solution in arriving at (3.16) and in the eigenfunction construction in deriving (4.3). However it is not obvious that conditions (2.19) are indeed satisfied by the solutions (3.26) and (3.30) which requires

$$\sum_{n=-2}^{\infty} \frac{(\nu_1 l^2 + k_n^2) Y_n'(0)}{C_n} Y_n(y) = 2 \sum_{n=-2}^{\infty} \frac{k_n(\nu_1 l^2 + k_n^2)}{K'(k_n)} \cosh \gamma_n (y+h) = 0.$$

This follows from consideration of the integral

$$I_4 = \frac{1}{2\pi i} \oint \frac{(\nu_1 l^2 + \alpha^2)\alpha \cosh \gamma (y+h)}{K(\alpha)} d\alpha$$

where as before, the contour is a circle, centre the origin of radius R and where again the integrand is $O(\alpha^{-3})$ on R as $R \to \infty$ and is odd in α. Thus, using familiar arguments,

$$I_4 = 2 \sum_{n=-2}^{\infty} \frac{k_n(\nu_1 l^2 + k_n^2)}{K'(k_n)} \cosh \gamma_n (y+h) = 0$$

as required.

REFERENCES

Andronov, I., Belinsky, B.P. & Dauer, D.P., 1996, Acoustic scattering by a narrow crack in an elastic plate. *Wave Motion*, **24**, 101–115.

Balmforth, N.J. & Craster, R.V., 1999, Ocean waves and ice sheets. *J. Fluid Mech.*, **395**, 89–124.

Chung, H. & Fox, C., 2002, Calculation of wave-ice interaction using the Wiener-Hopf technique. *New Zealand J. Math.*, in press.

Evans, D.V. & Davies, T.V., 1968, Wave-ice interaction. *Report No. 1313, Davidson Lab – Stevens Institute of Technology, New Jersey.*

Fox, C. & Chung, H., 1998, Green's function for forcing of a thin floating plate. *Tech. Report,* Vol 408, Department of Mathematics, University of Auckland, New Zealand. `http://www.math.aukland.ac.nz/Research/DeptRep/reports.html`

Fox, C. & Squire, V.A., 1990, Reflection and transmission characteristics at the edge of shore fast sea ice. *J. Geophys. Res.*, **95**(C7), 1,629–39.

Fox, C. & Squire, V.A., 1991, Coupling between an ocean and an ice shelf. *Ann. Glaciol.*, **15**, 101–8.

Fox, C. & Squire, V.A., 1994, On the oblique reflexion and transmission of ocean waves from shore fast sea ice. *Phil. Trans. R. Soc. A*, **347**(1682), 185–218.

Kouzov, D.P., 1963a, Diffraction of a plane hydro-acoustic wave on the boundary of two elastic plates. *P.M.M.*, **27**, 541-546.

Kouzov, D.P., 1963b, Diffraction of a plane hydro-elastic wave at a crack in an elastic plate. *P.M.M.*, **27**, 1037-1043.

Lawrie, J.B. & Abrahams, D., 1999, An orthogonal relation for a class of problems with high-order boundary conditions; applications in sound-structure interaction. *Quart. J. Mech. Appl. Math.*, **52**, 161–181.

Lawrie, J.B. & D. Abrahams, D., 2002, On the propagation and scattering of fluid-structural waves in a three-dimensional duct bounded by thin elastic walls. *Proc. IUTAM Symp. Manchester, UK.* Kluwer Academic Publishers, 279–288.

Marchenko, A.V., 1993, Surface wave diffraction at a crack in sheet ice. *Fluid Dynamics*, **28**, 230–237.

Marchenko, A.V., 1997a, Flexural gravity wave diffraction at linear irregularities in sheet ice. *Fluid Dynamics*, **32**, 548–560.

Marchenko, A.V., 1997b, Resonance interactions of waves in an ice channel. *J. Appl. Math. Mech.*, **61**, 931–940.

Marchenko, A.V., 1999, Parametric excitation of flexural-gravity edge waves in the fluid beneath an elastic ice sheet with a crack. *Eur. J. Mech. B/Fluids*, **18**, 511–525.

Sahoo, T., Yip, T.L. & Chwang, A.T.,, 2001, Scattering of surface waves by a semi-onfinite floating elastic plate. *Physics of Fluids*, **13**(11), 3215–3222.

Squire, V.A., 1994a, Sea Ice. *Sci. Prog. Oxford*, **69**, 19–43.

Squire, V.A., 1994b, A theoretical, laboratory and field study of ice-coupled waves. *J. Geophys. Res.*, **89**(C5), 8069–79.

Squire, V.A., 1994c, On the critical angle for waves entering shore fast ice. *Cold Reg. Sci. Tech.*, **10**(1), 59–68.

Squire, V.A., 1994d, How waves break up inshore fast ice. *Polar Rec.*, **22**(138), 281–5.

Squire, V.A., Dugan, J.P., Wadhams, P., Rottier, P.J., & Liu, A.K., 1995, Of ocean waves and ice sheets. *Ann. Rev. Fluid Mech.*, **27**, 115–168.

Squire, V.A. & Dixon A.W.,, 2000, An analytic model for wave propagation across a crack in an ice sheet. *Int. J. Offshore & Polar Eng.*, **10**, 173–176.

Teng, B., Cheng, L., Liu S.X. & Li, F.J., 2001, Modified eigenfunction expansion methods for interaction of water waves with a semi-infinite elastic plate. *Appl. Ocean Res.*, **23**, 357–368.

Tkacheva, L.A., 2001a, Scattering of surface waves by the edge of a floating elastic plate. *J. Appl. Mech. Tech. Phys.*, **42**, 638–646.

Tkacheva, L.A., 2001b, Hydroelastic behavior of a floating plate in water. *J. Appl. Mech. Tech. Phys.*, **42**, 991–996.

Tkacheva, L.A., 2001c, Surface wave diffraction on a floating elastic plate. *Fluid Dynamics*, **36**, 776–789.